Modified Laplacian pyramid for faster radiography image processing

Vladimir Ostojić, Đorđe Starčević, Vladimir Petrović, Siniša Suzić and Tijana Delić

***Abstract*—In this paper we present a Laplacian pyramid construction method that uses four coefficient kernel. This approach is motivated by the possible processing time reduction compared to the standard five coefficient kernel approach. The method was evaluated on clinical medical images, as a part of a radiography image processing framework. Results were compared to the ones obtained with the standard Laplacian pyramid. Experimental evaluation shows that comparable results can be obtained without introducing processing artifacts. It was shown that this approach uses 50 % less operations than the original one. Even when compared to an advanced binomial processing scheme, it was shown that operation count reduction of 12.5 % can be achieved.**

***Index Terms*—Digital radiography, Laplacian pyramid, medical image processing, multi-scale processing**

I. Introduction

DIGITAL radiography images are obtained by flat panel detectors (FPD) which have a response that is linearly proportional to the incidental x-ray intensity [1]. This results in very low contrast in unprocessed images, making them practically unusable for radiologists. An example image demonstrating the previous statement is shown in Fig. 1. Image appearance can be improved through the use of image processing algorithms.

Radiography image processing algorithms should address several issues. Image contrast should be enhanced in a manner that allows the radiologist to distinguish the density differences between different anatomies and structural differences within one anatomy. Detail visibility should be enhanced to a level that allows differentiation of small structures as they can potentially be malignant. Including noise reduction should be considered as enhancement algorithms tend to increase the noise prominence in the images [2]. Finally, radiography images are large in size (around 9 megapixels for diagnostic x-ray [3] and 12 to 25 megapixels for digital mammography, depending on detector size [4]) thus the processing speed is a practical concern that must be addressed.

Fig. 1. Example unprocessed image.

Multi-scale approaches for radiography image processing have attracted the attention of the community in the past decades. Authors of [5] proposed Laplacian pyramid (LP) [6] image decomposition and nonlinear mapping of the pyramid pixel values for image contrast amplification. Another LP based algorithm was proposed in [7]. This approach uses nonlinear mapping of pyramid pixels and proposes density and local activity adaptive processing for noise containment. Mammography image contrast enhancement through discrete dyadic wavelet transformation was proposed in [8]. Another wavelet based approach for chest radiographs enhancement was proposed in [9]. Nonlinear nature of the coefficient mapping, both for LP and the wavelet approaches, produces artifacts. These artifacts were addressed in [10]–[12]. Solutions for processing artifacts reduction were proposed in [13] and [14]. Comparison of LP and wavelet transform approaches showed that nonlinear mapping of LP produces less processing artifacts [15].

In each of the previously mentioned image processing approaches only noise and enhancement objectives were addressed, without serious consideration of processing time reduction. In this paper we analyze the LP that is constructed using a four coefficient filter instead of the standard five

Vladimir Ostojić is with the University of Novi Sad, Faculty of technical sciences, Trg D. Obradovića 6, 21000 Novi Sad, Serbia (e-mail: vladimir.ostojic@uns.ac.rs).

Đorđe Starčević is with the University of Novi Sad, Faculty of technical sciences, Trg D. Obradovića 6, 21000 Novi Sad, Serbia (e-mail: djordje.starcevic@uns.ac.rs).

Vladimir Petrović is with the University of Novi Sad, Faculty of technical sciences, Trg D. Obradovića 6, 21000 Novi Sad, Serbia (e-mail: vladimir.petrovic@uns.ac.rs).

Siniša Suzić is with the University of Novi Sad, Faculty of technical sciences, Trg D. Obradovića 6, 21000 Novi Sad, Serbia (e-mail: sinisa.suzic@uns.ac.rs).

Tijana Delić is with the University of Novi Sad, Faculty of technical sciences, Trg D. Obradovića 6, 21000 Novi Sad, Serbia (e-mail: tijanadelic@uns.ac.rs).

coefficient one, motivated by possible processing time reduction. Although it is noted that processing artifacts can be avoided (or reduced to a satisfactory level) by standard LP approaches [15], the conclusion might not stand for the proposed approach. For the purpose of validation, the new approach was embedded into a radiography image processing framework. Results were compared to the ones produced by the same framework using standard LP.

Section II explains the Laplacian pyramid construction algorithm. Constraints imposed on the low-pass filter used for the pyramid construction are outlined in Section III. Selection of coefficient values for the proposed filter and the obtained processing time reduction are analyzed in Section IV. Radiography image processing framework used for evaluation is explained in Section V. Results obtained on clinical images are outlined in Section VI. Section VII concludes the paper.

II. Laplacian pyramid

LP was originally proposed in [6] as a method for image compression. Pseudo code that depicts the process of LP calculation is shown in Fig. 2 where N is the number of pyramid layers, and i denotes the ordinal number of the layer.

Input: $original\ image\ I$
1: $GP_0 \leftarrow\ I$
2: $lpf \leftarrow\ low-pass\ filter\ kernel$
3: **for** $i = 0$ to $N-1$ **do**
4: $\quad GP_{i+1} = convolution(GP_i, lpf)$
5: $\quad GP_{i+1} = downsample(GP_{i+1})$
6: $\quad \widehat{GP_i} = upsample(GP_{i+1})$
7: $\quad \widehat{GP_i} = convolution(\widehat{GP_i}, lpf)$
8: $\quad LP_i = GP_i - \widehat{GP_i}$
9: **end for**
10: $Res = GP_N$

Fig. 2. Laplacian pyramid pseudo code.

First step in LP construction is low-pass image filtering as the preprocessing step for image downsampling. First LP layer is an image that represents the difference between the original image and its low-pass filtered and downsampled version. As the downsampled image size does not correspond to the original image size, the image will be upsampled before subtracting from the original image. Downsampled image can be further low-pass filtered and downsampled, allowing the repetition of the previously explained process of LP layer construction. In this way, a sequence of different sized images is obtained. As the algorithm uses downsampling by a factor of 2, every image in the sequence will have 4 times less pixels than the previous one (2 times less for each image axis). This size change is the reason why the sequence is called a pyramid. It should be noted that the sequence of the low-pass filtered and downsampled images also forms a pyramid which is called the Gaussian pyramid (GP). By convention, first layer of the GP is the original image. Thus, the LP is a sequence of error images, each being the difference between two layers of the GP.

Original image can be reconstructed from the LP and the last layer of the GP, which will be called the residual image, Res. Pseudo code that explains the original image reconstruction is shown in Fig. 3. Adding the last LP layer to an upsampled residual image will produce the second to last GP layer. This process can be repeated iteratively, leading to the perfect reconstruction of the original image.

1: **for** $i = N-1$ to 0 **do**
2: $\quad Res = upsample(Res)$
3: $\quad Res = convolution(Res, lpf)$
4: $\quad Res = Res + LP_i$
5: **end for**

Fig. 3. Original image reconstruction pseudo code.

Only one low-pass filter is used in the process of image decomposition and image reconstruction, and its characteristics are analyzed in Section III. Our objective is to investigate the repercussions of substituting the standard 5x5 filter with an 4x4 coefficient filter.

Every image in the LP can be interpreted as image that represents details of different scales. Various radiography image enhancement algorithms are based on this assumption [5], [7]. In this paper we used the reference processing framevork from [14], explained in section V.

III. Low-pass filter design

In the original LP paper [6] authors propose 5x5 spatial filter. This filter is separable, i.e. can be obtained as a convolution of one row (or column) filter and its transposed version. This filter was designed as a generating kernel $w(x)$ in a hierarchical discrete correlation (HDC) scheme proposed in [16]. Purpose of this algorithm is to aid the computation of local signal properties through correlation with different sized operators. Author proposes an iterative procedure:

$$\begin{aligned} g_0(x) &= f(x) \\ g_t(x) &= \sum_{i=-m}^{m} w(i) g_{t-1}(x + ir^{t-1}), \quad t > 1 \end{aligned} \tag{1}$$

where r, a positive integer, is the order of hierarchical correlation. Iteration t determines the layer $g_t(x)$ in the HDC hierarchy of input image $f(x)$. Kernel $w(i)$ has length $k = 2m+1$, i.e. kernel size is odd.

Constraints imposed on generating kernel $w(i)$ are:

- normalization $\sum_{i=-m}^{m} w(i) = 1$
- symmetry $w(x) = w(-x)$ for all x

- unimodality $w(x_1) \geq w(x_2) \geq 0$ for $0 \leq x_1 \leq x_2$
- equal contribution $\sum_{i=-m}^{m} w(j+ir) = \text{constant } (= 1/r)$, for all $j,\ 0 \leq j < r$

Equal contribution constraint ensures that every sample in the original sequence $f(x)$ contributes with equal weight to every $g_t(x)$ of the HDC.

For generating kernel of even width the definition of HDC (1) is modified:

$$\begin{aligned} g_0(x) &= f(x) \\ g_t(x) &= \sum_{i=-m}^{m-1} w(i+\frac{1}{2}) g_{t-1}(x + (i+\frac{1}{2}) r^{t-1}), \quad t > 1 \end{aligned} \tag{2}$$

Generating kernel $w(x)$ is defined at intermediate values, i.e. $x = ..., -1/2, 1/2, 3/2, ...$ If $(r^t - 1)/(r-1)$ is even, $g_t(x)$ is defined for integer x, and if not, it is defined at intermediate values like the $w(x)$. It should be noted that in this paper we will use $r = 2$ (as it is used for pyramids), thus $g_t(x),\ t > 0$ will always be defined at intermediate values.

Constraints imposed on the even generating kernel are the same as for the odd one. For kernel of width 4:

$$\begin{aligned} &w(-\frac{1}{2}) = w(\frac{1}{2}) = a \\ &w(-\frac{3}{2}) = w(\frac{3}{2}) = b \\ &2a + 2b = 1 \\ &a \geq b \geq 0 \end{aligned} \tag{3}$$

This leads to [16]:

$$\begin{aligned} b &= \frac{1}{2} - a \\ a &\in [\frac{1}{4}, \frac{1}{2}] \end{aligned} \tag{4}$$

As seen from (4), a is a free parameter that can be chosen form a set of values.

IV. Kernel coefficient value selection

It was shown in [17] that the use of the binomial kernels can significantly reduce the computational burden for pyramid calculation in comparison to the originally proposed kernels [6]. Substitution of the original kernel with a binomial $\widehat{K}_5(n)$ was proposed:

$$\begin{aligned} \widehat{K}_5(n) = \frac{1}{16}(&\delta(x) + 4\delta(x-1) + 6\delta(x-2) \\ &+4\delta(x-3) + \delta(x-4)) \end{aligned} \tag{5}$$

where $\delta(x)$ is the signal with unit value for $n = 0$ and zero value for $n \neq 0$.

Operations count reduction was achieved through successive addition of image pixels values as the binomial kernel can be obtained through repeated convolution of the two coefficient kernel $\widehat{K}_2(n)$:

$$\begin{aligned} K_2(n) &= \begin{cases} 1, & n = 0 \\ 1, & n = 1 \\ 0, & \text{otherwise} \end{cases} \\ \widehat{K}_2(n) = \frac{1}{2} K_2(n) &= \begin{cases} \frac{1}{2}, & n = 0 \\ \frac{1}{2}, & n = -1 \\ 0, & \text{otherwise} \end{cases} \end{aligned} \tag{6}$$

Note that kernel $\widehat{K}_2(n)$ is the normalized version of the binomial kernel $K_2(n)$. Convolution with $\widehat{K}_2(n)$ corresponds to addition of adjacent sample values (convolution with $K_2(n)$) and normalization through multiplication with $\frac{1}{2}$. Thus, filtering some signal $x(n)$ with $\widehat{K}_m$, where $m \geq 2$ represents the number of normalized binomial kernel coefficients, can be expressed in an iterative way:

$$\begin{aligned} &x_1(n) = x(n) \\ &x_i(n) = x_{i-1}(n) * K_2(n) \\ &x(n) * \widehat{K}_m = (\frac{1}{2})^{(m-1)} x_m(n) \end{aligned} \tag{7}$$

Motivated by the previous, we investigate a four coefficient kernel:

$$\widehat{K}_4(n) = \frac{1}{8}(\delta(x) + 3\delta(x-1) + 3\delta(x-2) + \delta(x-3)) \tag{8}$$

It should be noted that $\widehat{K}_4(n)$ is a valid generating kernel for the DHC. Normalization, unimodality and symmetry constraints are satisfied by design. Proving the equal contribution property can be done through setting the value $a = 0.375$ in (4). It is interesting to note that the generating kernel analysis in [16] showed that setting a to approximately 0.37 will produce a result most similar to the Gaussian filter.

Number of additions in this approach is the same as when filtering with a generating kernel. This approach, however, does not perform multiplications, except the one used for normalization. This multiplication can be done after all of the convolutions, as shown in (7). In this way, only one multiplication is used per signal sample in contrast to five used in the original approach. For image processing, this filtering is done twice, as the 2D kernel is separable. If the normalization multiplication is done after the convolution processing, only one multiplication can be done instead of two (one for each 1D kernel). Hence, proposed approach uses 50 % less operations per pixel that the original one, that is 8 additions (4 for each 1D filtering) and one multiplication for normalization instead of 8 additions and 10 multiplications (4 additions and 5 multiplications for each 1D filtering).

As explained, binomial filtering uses less operations than the original approach. Therefore, we compare binomial kernels whose widths are four and five. Number of operations performed in filtering using the even kernel is 12.5 % lower compared to using the odd one because the number of additions per image axis is decremented by 1. It should be noted that this implementation requires iterative memory readouts as each convolution is calculated based on the result of a previous one. This might be impractical if memory readout speed is low compared to processor clock speed. In such case, one could use an implementation based on the "multiply–accumulate" operation common in digital signal processing, or use a straightforward implementation that uses coefficients listed in (5) or (8). Even then, the reduction of 20 % in the number of operations is still present as the even kernel has one coefficient less.

V. Radiography image processing

Radiography image processing algorithm used in our research is composed of several steps and corresponds to the reference framework presented in [14]. The firsts processing step is high dynamic range compression of the unprocessed image. Logarithm operator was chosen for the compression task as it produces the image in which the pixel intensity is inversely proportional to anatomy density. LP decomposition was used as the basis for detail amplification and contrast enhancement. LP coefficients from different layers were mapped using the sigmoidal function:

$$\widehat{LP_i}(x,y) = C_i\left(\frac{1}{1+e^{-k_i LP_i(x,y)}} - \frac{1}{2}\right) \tag{9}$$

where $LP_i(x,y)$ are the LP coefficients at layer i, x and y are the spatial coordinates, $\widehat{LP_i}(x,y)$ are the enhanced LP coefficients, C_i and k_i are constants that depend on the pyramid layer level.

This approach increases the value of the low absolute value coefficients, corresponding to detail enhancement for lower level LP layers, and to local contrast enhancement for higher level layers. Another useful characteristic of the sigmoidal function is that the high absolute value coefficients will be reduced, resulting in additional local contrast enhancement. Very low value LP coefficients were omitted in the enhancement process to avoid noise amplification [14].

VI. Evaluation and results

To evaluate the results obtained with even and odd kernels, a set of 47 clinical radiography images was used. Images were acquired using Varian PaxScan4343 FPD with square pixels of length 139 μm. Each images size is 3072 x 3072 pixels.

Images show various anatomies (hand, leg, chest, head, spine etc.) from different patients obtained during regular clinical routine. Example images are shown in Fig. 4, Fig. 5 and Fig. 6.

As shown, images processed using even and odd kernels are very similar to each other. No significant difference in detail visibility or contrast was found on the whole evaluation set.

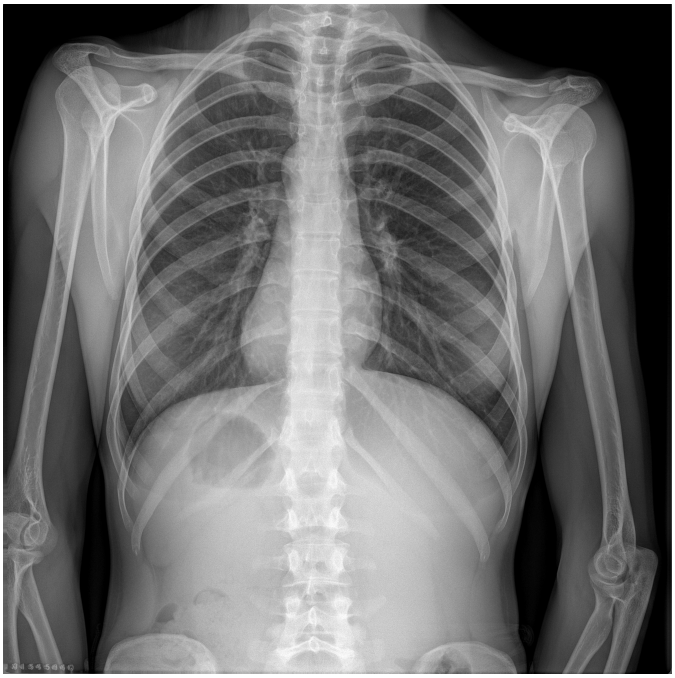

(a)

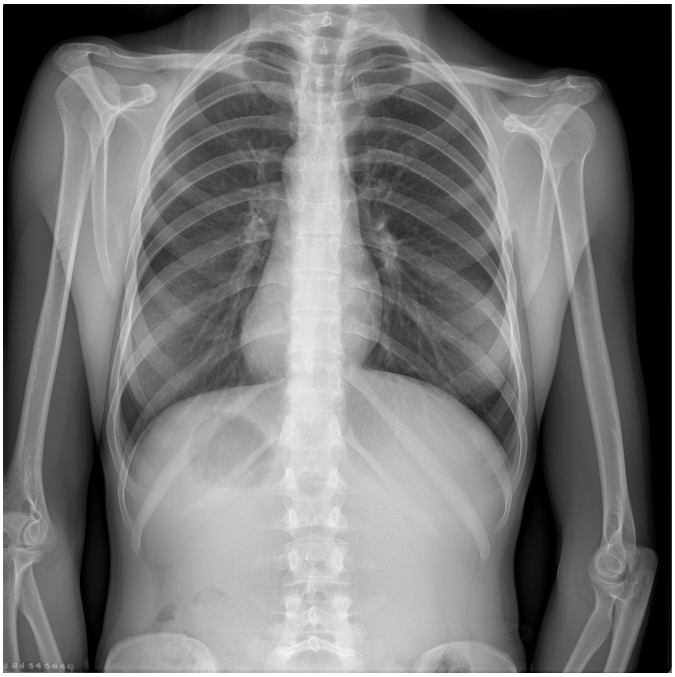

(b)

Fig. 4. Example chest image processed with (a) four and (b) five coefficient filter.

It was found that there is also no difference in the noise prominence. Minor differences between processed images are expected as the used kernels have different characteristics. As can be seen, proposed approach does not introduce processing artifacts, thus has a potential to be a part of a radiography

(a)

(b)

Fig. 5. Example knee image processed with (a) four and (b) five coefficient filter.

(a)

(b)

Fig. 6. Example spine image processed with (a) four and (b) five coefficient filter.

image processing framework. Result are promising, however an observer study that involves trained medical personnel is needed for detailed evaluation.

VII. Conclusion

In this paper we presented an LP construction method that uses four coefficient kernel instead of the five coefficient one. It was shown that this approach uses 50 % less operations than the original approach, and 12.5 % less operations in comparison to the five coefficient binomial kernel approach. Even in the ”naive” implementation (”multiply-accumulate”), 20 % less operation are used.

Proposed LP was evaluated as a basis for multi-scale radiography image processing. Results were compared to the ones obtained with the LP that uses standard five coefficient kernel. Experimental results show that image contrast and detail visibility are comparable. Noise prominence was not amplified and no processing artifacts were introduced.

Acknowledgment

This research is supported by grants TR32040 and TR32035 of Serbian Ministry of Science.

REFERENCES

[1] A. J. Seibert, "Flat-panel detectors: how much better are they?" *Pediatric Radiology*, vol. 36, no. 2, pp. 173–181, 2006.

[2] M. Couwenhoven, W. Sehnert, X. Wang, M. Dupin, J. Wandtke, S. Don, R. Kraus, N. Paul, N. Halin, and R. Sarno, "Observer study of a noise suppression algorithm for computed radiography images," in *Proc. SPIE*, vol. 5749, pp. 318–327, 2005. [Online]. Available: http://dx.doi.org/10.1117/12.595159

[3] E. L. Nickoloff, "Aapm/rsna physics tutorial for residents: Physics of flat-panel fluoroscopy systems," *RadioGraphics*, vol. 31, no. 2, pp. 591–602, 2011. [Online]. Available: http://dx.doi.org/10.1148/rg.312105185

[4] M. J. Yaffe, "Detectors for digital mammography," in *Digital Mammography*, U. Bick and F. Diekmann, Eds. Berlin, Heidelberg: Springer Berlin Heidelberg, pp. 13–31, 2010. [Online]. Available: http://dx.doi.org/10.1007/978-3-540-78450-0_2

[5] P. Vuylsteke and E. P. Schoeters, "Multiscale image contrast amplification (musica)," in *Proc. SPIE*, vol. 2167, pp. 551–560,1994. [Online]. Available: http://dx.doi.org/10.1117/12.175090

[6] P. Burt and E. Adelson, "The laplacian pyramid as a compact image code," *IEEE Transactions on Communications*, vol. 31, no. 4, pp. 532–540, Apr 1983.

[7] M. Stahl, T. Aach, T. M. Buzug, S. Dippel, and U. Neitzel, "Noise-resistant weak-structure enhancement for digital radiography," in *Proc. SPIE*, vol. 3661, pp. 1406–1417, 1999. [Online]. Available: http://dx.doi.org/10.1117/12.348539

[8] A. Laine, J. Fan, and W. Yang, "Wavelets for contrast enhancement of digital mammography," *IEEE Engineering in Medicine and Biology Magazine*, vol. 14, no. 5, pp. 536–550, Sep 1995.

[9] J. P. Bolet, A. R. Cowen, J. Launders, J. Davies, G. J. S. Parkin, and R. F. Bury, "Progress with an "all-wavelet" approach to image enhancement and de-noising of direct digital thorax radiographic images," in *1997 Sixth International Conference on Image Processing and Its Applications*, vol. 1, pp. 244–248, Jul 1997.

[10] L. J. Cesar, B. A. Schueler, F. E. Zink, T. R. Daly, J. P. Taubel, and L. L. Jorgenson, "Artefacts found in computed radiography," *The British Journal of Radiology*, vol. 74, no. 878, pp. 195–202, 2001. [Online]. Available: http://dx.doi.org/10.1259/bjr.74.878.740195

[11] S. L. Solomon, R. G. Jost, H. S. Glazer, S. S. Sagel, D. J. Anderson, and P. L. Molina, "Artifacts in computed radiography," *American Journal of Roentgenology*, vol. 157, no. 1, pp. 181–185, 1991.

[12] A. Walz-Flannigana, D. Magnuson, D. Erickson, and B. Schueler, "Artifacts in digital radiography," *American Journal of Roentgenology*, vol. 198, no. 1, pp. 156–161, 2012.

[13] M. Maitre, Y. Chen, and F. Tong, "High-dynamic range compression using a fast multiscale optimization," in *2008 IEEE International Conference on Acoustics, Speech and Signal Processing*, pp. 541–544, March 2008.

[14] V. Ostojić, D. Starčević, and V. Petrović, "Artifact reduction in multiscale contrast enhancement for digital radiography," in *2014 22nd Telecommunications Forum Telfor (TELFOR)*, pp. 513–516, Nov 2014.

[15] S. Dippel, M. Stahl, R. Wiemker, and T. Blaffert, "Multiscale contrast enhancement for radiographies: Laplacian pyramid versus fast wavelet transform," *IEEE Transactions on Medical Imaging*, vol. 21, no. 4, pp. 343–353, April 2002.

[16] P. J. Burt, "Fast filter transform for image processing," *Computer Graphics and Image Processing*, vol. 16, no. 1, pp. 20 – 51, 1981. [Online]. Available: http://www.sciencedirect.com/science/article/pii/0146664X81900927

[17] R. A. Haddad and A. N. Akansu, "A class of fast gaussian binomial filters for speech and image processing," *IEEE Transactions on Signal Processing*, vol. 39, no. 3, pp. 723–727, Mar 1991.